



SIMULATION OF SOIL DYNAMIC COMPACTION

A. Rouaiguia¹ & R. Al-Zahrani¹

1: Assistant Professor, Department of technical construction, Abha College of Technology

ABSTRACT

Dynamic compaction is the process used to densify loose deposits of cohesionless soils by means of high energy impact. Generally speaking, the improvement of soils is achieved by dropping a heavy mass ranging between 10 and 40 tonnes from a height varying between 10 and 25 meters onto pretermind grid points on the ground.

This paper describes numerical simulation study of dynamic compaction process by using [Lusas[®], 2000] to generate a full axisymmetric elasto-plastic finite element representation of the soils. The cylindrical poulder (damp) is modeled as a rigid body impacting collision onto the soil and it is 1 meter in length and has a diameter of 2.5 meters. Compared results such as poulder penetration during the process, drop mass effects, Young's modulus, density, cohesion of the soil and peak particle velocity attenuation from different depths are well presented. The numerical results are quite consistent with published data.

Keywords: *Lusas, numerical analysis, dynamic compaction, soil behavior, impacting poulder, peak particle velocity.*

1. INTRODUCTION

During the last several years, dynamic compaction has become popular as a ground improvement process for compacting and strengthening loose or soft soils to support buildings, roadways, and other heavy construction. The method involves the systematic dropping of a large steel or heavy concrete mass varying from 10 to 40 tonnes, and from a height generally varying between 10 and 25 meters onto predetermined grid points on the ground. When the damper strikes the ground, vibrations are transmitted to varying distances from the point of impact. These vibrations are usually negligible for sites where boundaries and buildings are at relatively large distances from the source of impact. However, when tamping is done near the edges of the property in developed areas, ground vibrations can be transmitted into adjacent facilities and in some instances may cause significant biological annoyance or structural damage. Therefore one of the most common limitation of dynamic compaction is the effect of ground vibration on adjacent facilities.

The high-energy ground vibrations produced by dynamic compaction can be felt over significant distances (up to 20 meters) and can be damaging to nearby structures [Rollins et al., 1999]. Current guidance is based on observations of the effects of peak particle velocities on structures. For many years, a limiting peak particle velocity of 50 mm/s has been considered the structural damage criteria for one or two-story buildings. The primary sources of data for this basis came from blasting records from surface mining operations near residential communities [Mayne, 1985]. However, ground vibrations caused from dynamic compaction operations are unique from another types of construction activity, such as blasting, pile driving, and traffic. Generally speaking, the performance design and application of dynamic compaction are, however, still largely empirical in nature, relying heavily on the designer's experience and judgment. A pilot test is often carried out at the site to ascertain the operational parameters, so as to minimize the operational costs [Chow et al., 1992]. An improved empirical approach with selected parameters for dynamic compaction has been recently suggested [Lo et al., 1990].

The highly complicated soil response during high-energy impact is still not properly understood. The dynamic compaction process generally has not progressed far beyond providing practical solutions with performance monitoring through the use of in-situ tests which are not capable of providing most of the operational parameters, such as the propagation of waves beneath the ground surface due to the difficulties in placing the geophones at depth. In addition, dynamic compaction may harmfully affect surrounding buildings within its effective distances from serious disturbances of working conditions for sensitive devices and people will be able to notice structural damages. Empirical equations employed for assessment of expected soil vibrations from construction and industrial sources usually allow only calculation of a vertical peak amplitude of vibrations and not always sufficiently accurate. These equations cannot incorporate specific differences of soil conditions at each site because heterogeneity and spatial variation of soil properties. These

factors can strongly affect characteristics of propagated waves in soil from construction and industrial vibration sources.

Nowadays, there is an overwhelming need for the formulation of a reliable predictive theory. This will not only give a better understanding of the mechanics of dynamic compaction but will also provide a means of studying the influencing parameters in a systematic manner leading to a more reliable determination of the operational parameters for estimating cost. Some researchers have studied dynamic compaction by using one dimensional model to simulate the soil behavior under high-energy impact [Scott & Pearce, 1975]. The model, however, appears to have found little practical application. The one-dimensional models of [Mayne & Jones, 1983] and [Holeyman, 1985] appear to have used largely to estimate impact stresses. The finite difference and boundary element models of [Oian, 1986], using an empirical soil model, were used to estimate the penetration of the poulder during impact. [Pan & Selby, 2000] has simulated the dynamic compaction of loose soils under dynamic loads.

2. NUMERICAL MODELLING

These examples show the analysis of a poulder dynamically impacting a soil. The problem is 2D axisymmetric about Y axis. The poulder is of a length of 1 meter and 2.5 meters in diameter. The impact velocity at the target soil is relating to the drop height. The analysis is materially nonlinear due to the plastic deformation in the soil and exhibits boundary condition nonlinearity due to its contact with the poulder. An elsto-plastic (optimized) Von Mises model is used for the poulder and an elasto-plastic Mohr-Coulomb is used for the soil analysis. 2D slidelines are used to specify the contact conditions between the base of the poulder and the top of the soil. Both the Mohr-Coulomb and Von Mises models are available in the library of Lusas within the material properties.

2.1 Soil Parameters

In order to compare soil parameters, different parameters have been used in this analysis, which are as follow:

a) Young's modulus,

$$E1= 5.0 \times 10^3 \text{ kPa}, \quad E2= 10.0 \times 10^3 \text{ kPa}, \quad E3= 12.0 \times 10^3 \text{ kPa}$$

b) Cohesion,

$$C1= 10 \text{ kPa} \quad , \quad C2= 15 \text{ kPa}, \quad C3= 20 \text{ kPa}$$

c) Mass density

$$\rho_1 = 1400 \text{ Kg/m}^3, \rho_2 = 1600 \text{ Kg/m}^3, \rho_3 = 1800 \text{ Kg/m}^3, \rho_4 = 2000 \text{ Kg/m}^3$$

Initial friction angle, $\phi = 25^\circ$, Poisson's ratio, $\nu = 0.35$

2.2 Pounder Impact parameters

The optimized elasto-plastic Von Mises model is used for the pounder. The use of the optimized Von Mises instead of the standard Von Mises model will significantly improve the speed of the solution for explicit dynamics.

Diameter, $D = 2.5 \text{ m}$; Length, $L = 1 \text{ m}$; Young's modulus, $E = 2.1 \times 10^6 \text{ kPa}$; Poisson's ratio, $\nu = 0.30$; Mass density, $\rho = 1040 \text{ Kg/m}^3$, Initial uniaxial yield stress, $\sigma_{y0} = 1.2 \times 10^3 \text{ kPa}$, Isotropic hardening gradient (hardening slope) = $1 \times 10^3 \text{ kPa}$, Maximum effective plastic strain = 1000.

The analysis is performed by prescribing the impact velocity of the pounder to the associated nodes at the initial condition. The impact velocity of the pounder to the associated nodes at the initial condition. The impact velocity can be obtained from the expression

$$V = \sqrt{2gH\xi} \quad V = \sqrt{2.g.H.\xi} ,$$

where V = impact velocity of the pounder; g = acceleration due to gravity; H = height of fall; and ($\xi=1$ for free fall). Some energy loss can be expected if the pounder is allowed by means of cable winch. In this study, a free mass is considered and the impact velocity was initiated by a vertical velocity of:

$$V = \text{Sqrt}(2.g.H.\xi) = \text{Sqrt}(2 \times 9.81 \times 11.5 \times 1) = 15 \text{ m/s}$$

The impact load of a mass of $M = 2700 \times (\pi \xi \times 2.5 \times 2.5) / 4 = 13.25 \text{ Mg}$.

The two-dimensional finite element representation for both the soil and impacting the pounder is shown in Figure1.

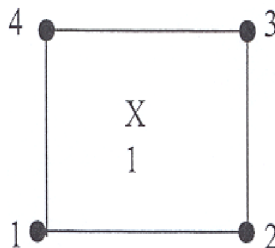


Figure 1. 2D Axisymmetric Solid Explicit Dynamic Element (Four nodes).

Due to symmetry, only one-half of the system is discretized. The left boundary represents the axis of rotational symmetry. The grid consists of 5041 nodes and 4900 quadrilateral elements for the soil and 18 nodes and 10 quadrilateral elements for the pounder as shown in Figure 2.

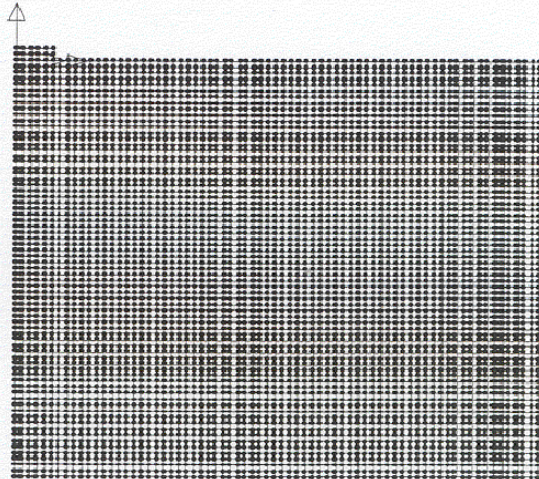


Figure 2. Finite Element Initial Mesh for soil and impact pounder.

The dimensions of the model were chosen to be 35 m by 35 m with the mesh increment has adopted to $\Delta x = 0.5$ m, and the time step was automatically generated by Lusas.

3. DISCUSSION

Figure 3 shows the finite element deformed mesh for soil after the application of impact pounder.

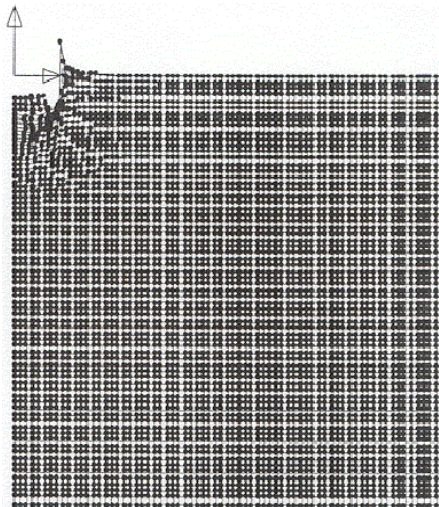


Figure 3. Finite Element Deformed Mesh for soil and Impact pounder

Figure 4 shows the finite element boundary conditions specified for this analysis. At the bottom and right sides of the soil domain, the soil is fixed in both directions. At the left side of the domain, both the soil and the poulder are free to move in the vertical direction and are fixed in the horizontal direction.

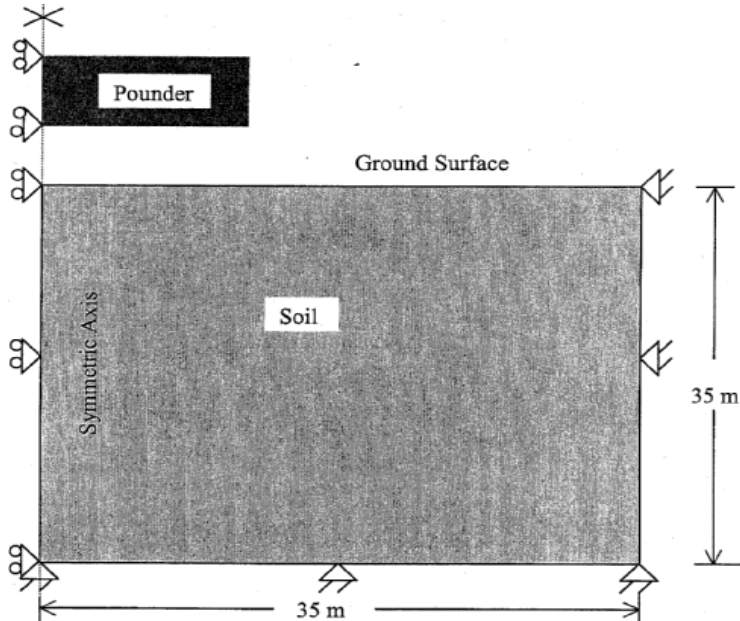


Figure 4. Soil and Poulder model boundary conditions

The variations of mass penetration (crater depth) versus depth at different soil cohesion are shown in figure 5, where the mass penetration was found to increase with low values of cohesion. As regards to figure 6, it has been concluded that soil density has no effect on the variations of mass penetration (crater depth).

The influence of Young's modulus on mass penetration was also evaluated. The mass penetration (crater depth) increased as the Young's modulus decreased as shown in figure 7.

Figure 8 summarizes the influence of drop mass on maximum drop mass (crater depth). The results indicate that the drop mass has a significant influence on the variations of crater depth, in which the crater depth increased with drop mass. The variations of crater depth with drop height are shown in figure 9. It should be noted that significant increase of crater depth with increasing drop height. Both drop height and drop mass show similar trend of increase with crater depth. As mentioned earlier and to compare the results of this study with [Pan & Selby, 2000], similar initial soil parameters were used. It is worth noticing that the estimated maximum mass penetration was 450 mm for drop weight of 10 Mg, which is between the two

values of 510 mm for the force-time load solution and 260 mm for the rigid body impact load analysis given by [Pan & Selby, 2000].

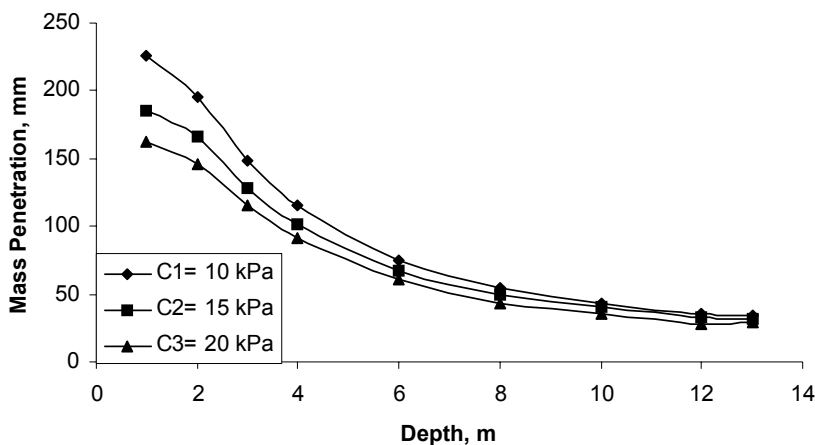


Figure 5. Mass Penetration versus Depth at different cohesion

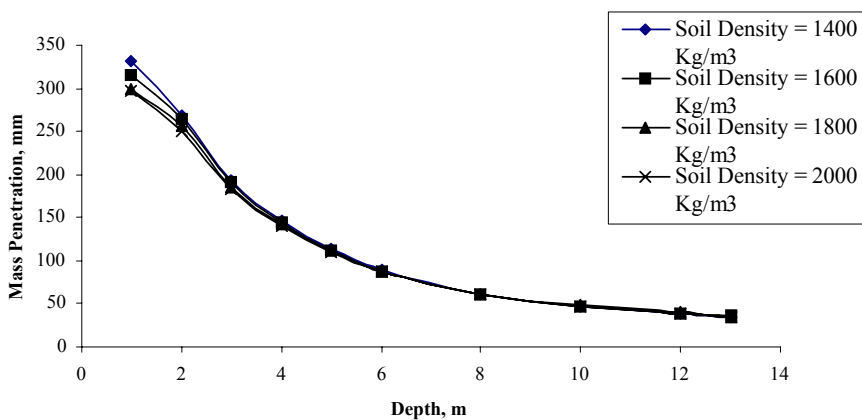


Figure 6. Mass Penetration versus Depth at different Soil Density

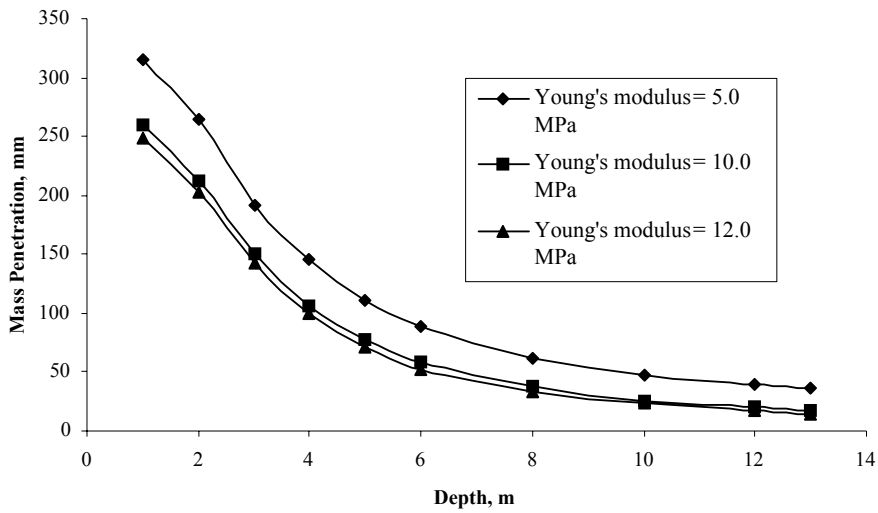


Figure 7. Mass Penetration versus Depth at different Young's Modulus

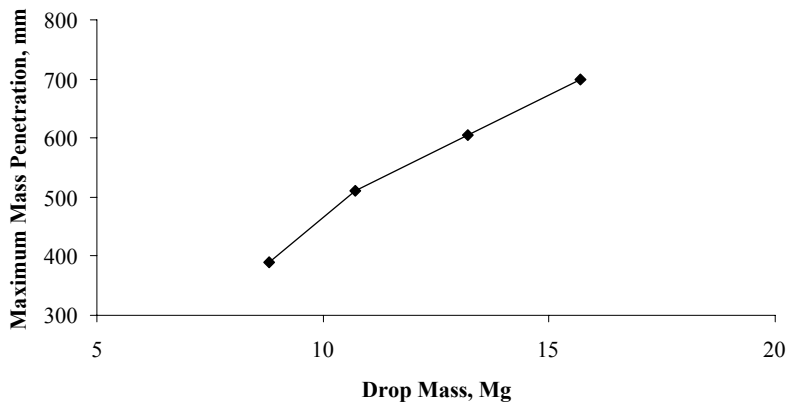


Figure 8. Drop Mass versus Maximum Mass Penetration

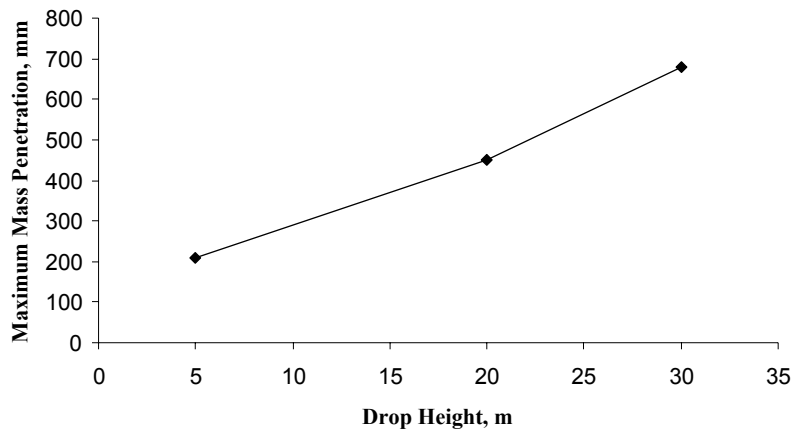


Figure 9. Drop Height versus Maximum Mass Penetration

4. CONCLUSION

The findings of this numerical study on ground vibrations caused by dynamic compaction of loose soils indicate that: the mass penetration (crater depth) due to dynamic compaction correlates well with the tamper mass, drop height, Young's modulus and soil cohesion. The penetration mass increases significantly as drop mass and drop height increase. However, the penetration mass decreases as Young's modulus and cohesion increase. These results are quite reasonable with some published data.

It is hoped that the program will contribute the basic understanding of complex field processes, and extend available design technologies. The result obtained from this study can contribute to field and laboratory situations such as: estimation of the effects of drop height, drop mass, and soil characteristics.

REFERENCES

1. Chow, Y.K., Yong, D.M., Yong, K.Y. and Lee, S.L., 1992, "Dynamic compaction analysis", *Journal of Geotechnical Engineering*, Vol. 118(8), pp 1141-1157.
2. Holeyman, A., 1985, "Unidimensional modellization of dynamic footing behavior", *Proceedings 11th Conference on Soil Mechanics and Foundation Engineering*, pp 761-764.
3. Lo, K.W., Ooi, P.L. and Lee, S.L., 1990, "Unified approach to ground improvement by heavy tamping", *Journal of Geotechnical Engineering*, ASCE, 116(3), pp 514-527.
4. Lusas., 2000, "Powerful Finite Element Technology for specialist applications", Version 13.2-2, FEA Ltd.

5. Mayn, P.W., 1985, "Ground vibrations during dynamic compaction", *Vibration problems in Geotechnical Engineering Proceedings. Proceedings of Symposium sponsored by the Geotechnical Engineering Division of ASCE, New York*, pp 247-265.
6. Mayne, P.W. and Jones, J.S., 1983, "Impact stresses during dynamic compaction", *Journal of Geotechnical Engineering, ASCE*, 109(10), pp 1342-1347.
7. Pan, J.L. and Selby, A.R., 2000, "Simulation of dynamic compaction of loose soils", *The Second International Conference on Engineering Computational Technology, Leuven, Belgium*.
8. Qian, J.H., 1986, "Dynamic consolidation from practice to theory", 8th *Asian Regional on Soil Mechanics and Foundation Engineering, Japanese Society for Soil Mechanics and Foundation Engineering*, 2, pp 213-217.
9. Rollins, K.M and Rogers, G.W., 1994, "Mitigation measure for small structure on collapsible alluvial soils", *Journal of Geotechnical Engineering, Vol. 120(9)*, pp 1533-1553.
10. Rollins, K.M., Osten, R. and Kim, J.H., 1999, "Deep dynamic compaction of collapsible soils", *XI Pana-American-Conference on Soil Mechanics and Geotechnical Engineering, Vol. 1*, pp 43-50.
11. Scott, R.A., Pearce, R.W., 1975, "Soil compaction by impact", *Geotechnique*, 25(1), pp 19-30.